Integrated Horn Antennas for Terahertz Applications

George V. Eleftheriades, Walid Y. Ali-Ahmad,
Linda P. Katehi and Gabriel M. Rebeiz

NASA/Center for Space Terahertz Technology
Electrical Engineering and Computer Science Department
University of Michigan
Ann Arbor, MI 48109-2122

SUMMARY

We are developing integrated and receivers antennas for terahertz applications. As the remote-sensing/radio-astronomical frequencies are pushed higher into the millimeter and submillimeter- wave regions, integrated antennas and receivers become competitive with standard waveguide receivers. The integrated receivers consist of an antenna integrated directly with a matching network/mixer. Integrated antennas and receivers are easier to manufacture, more reliable and much less expensive than waveguide receivers. The integration also allows the use of linear or two-dimensional arrays without a dramatic increase in cost.

The heart of an integrated receiver is the planar antenna and the antenna/mixer matching network. We have concentrated our efforts into the development and optimization of the high-efficiency integrated horn antenna (Fig. 1). The antenna consists of a dipole suspended in a pyramidal cavity etched in Silicon.The horn antennas are typically between 1λ and 1.5λ-square, and show excellent patterns at 93 GHz with a directivity around 10-12 dB. In the past year, we have achieved significant advance in the analysis and optimization of integrated horn antennas and the projects are summarized below:

1- Full-Wave Analysis of Dipole-Fed Horn Antennas. A rigorous procedure for evaluating the Green's function and input impedance of a dipole-fed horn antenna has been recently developed at the University of Michigan. The geometry of the horn structure is approximated by a cascade of rectangular waveguide sections, and the boundary conditions are matched at each of the waveguide sections and at the aperture of the horn. For the case of a single horn surrounded by an infinite metallic wall, the fields in space are given by a continuous spectrum of plane waves. The input impedance is calculated by solving the Pocklington's integral equation using the method of moments on the source interface.

The patterns for a 1.35λ-square horn in a ground-plane, and in a two-dimensional array are shown in Figure 2. The theoretical patterns agree very well with measured patterns at 92 GHz, and on microwave scale models at 3 GHz. The H-planes are smooth and similar

in both cases, due to the TE_{10} tapering of the electric field across the aperture. The E-plane patterns are much more interesting. The dipole couples to the TM_{12} and the TE_{12} waveguide modes, and their effect is to increase the vertical component at the center and to reduce it at the E-plane edges. The resultant pattern shows a near H- plane behavior near broadside, and levels off at -11dB for larger angles. In the case of the E-plane in a two-dimensional array, the horn sees the array and the spikes and nulls in the patterns are due to specific Floquet- modes. Impedance measurements were done on a microwave scale model at 1-2 GHz for a 1.35λ dipole-fed horn. The input impedance and resonant length are a strong function of the dipole position inside the cavity (Fig. 3), and vary from 40Ω to 170Ω and 0.37λ to 0.45λ, respectively. The dipole impedance for a feed position of 0.39λ is quite suitable for Schottky-diode receivers (Fig. 4). The horn has about 8% and 20% bandwidth for feed positions of 0.39λ and 0.6λ respectively. These bandwidths are adequate for most millimeter-wave applications.

2- Double-Polarized Antennas. A two-dimensional dual-polarized monolithic horn-antenna array has been designed for 92 GHz (Fig. 5). The antenna consists of two perpendicular dipoles suspended on the same membrane inside the horn cavity. The dipoles couple to an orthogonal set of waveguide modes, and therefore are effectively isolated from each other. The measured mutual coupling between the antennas on a microwave scale model was less than -30 dB. A design with an aperture of 1.35λ-square, and a feed position of 0.39λ was fabricated. The antennas are linearly polarized and a polarization isolation better than -23 dB was measured at 92 GHz (Fig. 6). The measured E & H-plane patterns agree well with theory and are virtually identical for both polarizations. Detailed analysis and experimental results are presented in the references.

3- 802 GHz Imaging Array. A 256-element imaging array has been fabricated and tested at 802 GHz (Fig. 7). The patterns agree very well with theory (Fig. 8), and the associated directivity for a 1.4λ horn aperture calculated from the measured E and H-plane patterns is $12.3 \pm 0.2dB$. The patterns show a main-beam efficiency of 88% in a 100°- beamwidth and are suitable for f/0.9 reflector systems. We would like to note that this result presents one of the best patterns measured on a planar antenna at frequencies higher than 500 GHz.

4- Step-Profiled Diagonal Horn Antennas. The main limitations of integrated horn antenna stem from their large flare angle of 70.6° which does not allow us to fabricate apertures greater than 1.5λ before the phase-errors becomes too large. This results in gains around 13 dB and 10-dB beamwidth of $90 - 95°$. We have investigated a new step-profiled horn which reduces the effective flare-angle of the horn to $30 - 40°$ and allows us to achieve gains between 17 and 20 dB (Fig. 9). The circular symmetry is also enhanced by positioning the exciting dipole along the diagonal of the horn. A specific step-profiled horn has been designed for millimeter-wave applications. The horn geometry has an effective flare-angle of 30° and an aperture size of 2.92λ. It is synthesized using 12 wafers each of thickness of 0.4λ. The step-size for each wafer discontinuity is 0.17λ. The calculated

E and H-plane patterns show a 10-dB beamwidth of 40° and a side-lobe level of -17 dB, with a directivity of 17.5 dB (Fig. 10). The 45° plane is effectively wider than either the E and H-planes, but matches them quite well up to the -10 dB points (Fig. 11). The step-profiled horn was also compared to a horn with a cavity defined by its smooth outer envelope and has the same aperture size. It is seen that the patterns match well up to -17 dB but then the step-profiled horn widens and develops a side-lobe (Fig. 12). Similar effects have been observed at the 45° planes. The measured patterns on a 12 GHz model of the smooth dipole-fed horn agree very well with theory. The calculated coupling efficiency of the step-profiled horn to a gaussian beam is around 75% and is approximately the same as a waveguide-fed pyramidal horn antenna.

We are now designing a hybrid Potter horn with a dipole-fed integrated horn cavity and a long machined phasing section. Preliminary results show a 20 dB gain hybrid-horn with a gaussian-beam coupling efficiency of 94%. Additional results and measurements will be presented in the coming CSTT symposium.

For additional information, the reader is referred to the following articles:

[1] G.M. Rebeiz, D P. Kasilingam, P.A. Stimson, Y. Guo and D.B. Rutledge, "Monolithic millimeter-wave two-dimensional horn imaging arrays," *IEEE Trans. Antennas Propag.*, vol. AP-28, Sept 1990.

[2] Y. Guo, K. Lee, P.A. Stimson, K. Potter and D.B. Rutledge, "Aperture Efficiency of Integrated-Circuit Horn antennas," *IEEE AP-S Intl. Symp.*, Dallas, Texas, May 7- 11, 1990.

[3] W.Y. Ali-Ahmad and G.M.Rebeiz, "92 GHz dual-polarized integrated horn antennas," To appear in the June 1991 Issue of the *IEEE Trans. Antennas Propag.*.

[4] W.Y. Ali-Ahmad and G.M. Rebeiz, H. Davee and G. Chin, "802 GHz integrated horn antennas imaging array," To appear in the May 1991 Issue of the *Intl. Journal Infrared and Millimeter Waves.*

[5] G.V. Eleftheriades, L.P. Katehi and G.M. Rebeiz, " High-gain step-profiled integrated horn antennas," To be presented at the *IEEE AP-S Symp.*, Ontario, Canada, June 24-27, 1991.

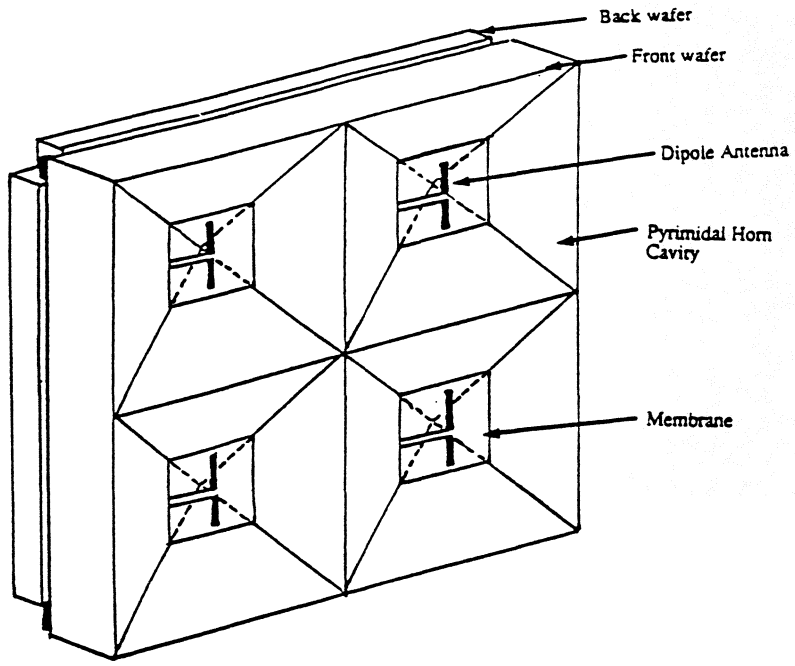

Figure 1: An integrated horn antenna with single polarization.

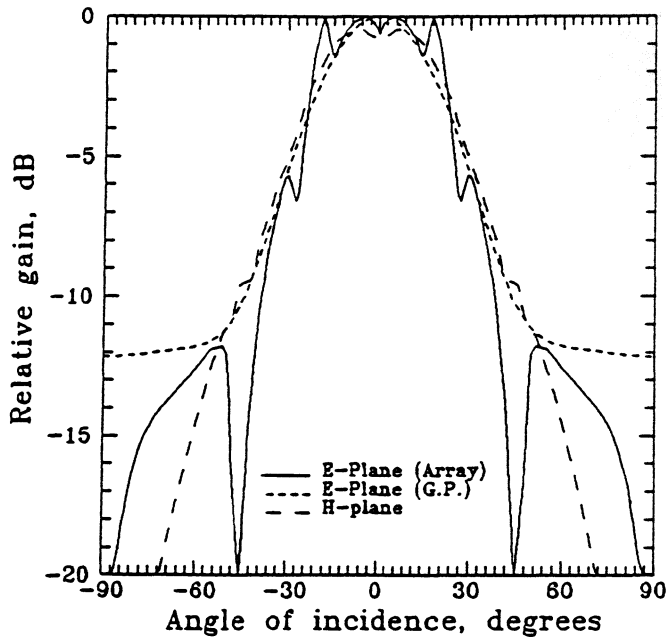

Figure 2: The E- and H-plane patterns of a 1.35λ horn antenna in a ground-plane and in a two-dimensional array. The theoretical agree very well with experiments at 3 GHz and 92 GHz.

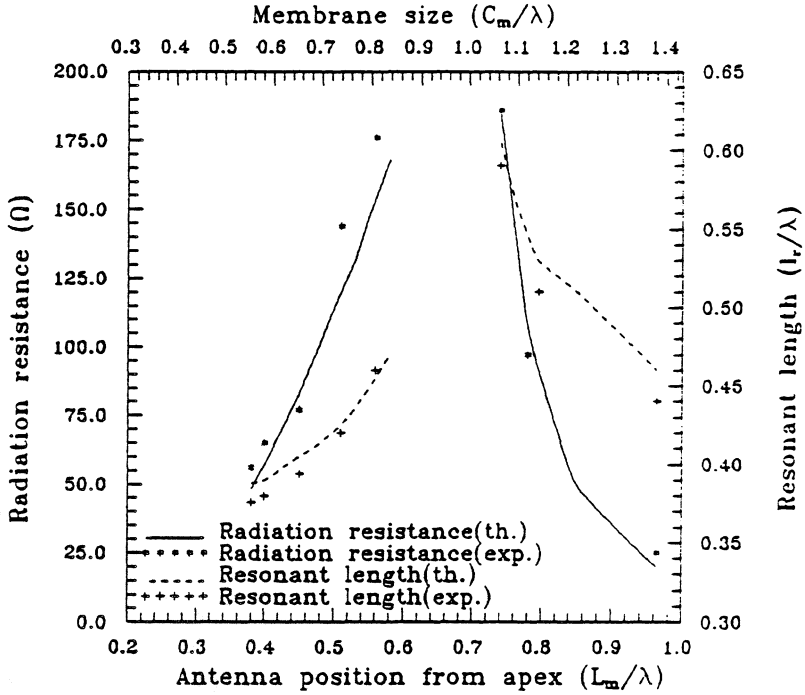

Figure 3: Measured and predicted dipole resonant resistance and resonant length vs. dipole position from the apex. Notice the region of no resonance in the center of the horn.

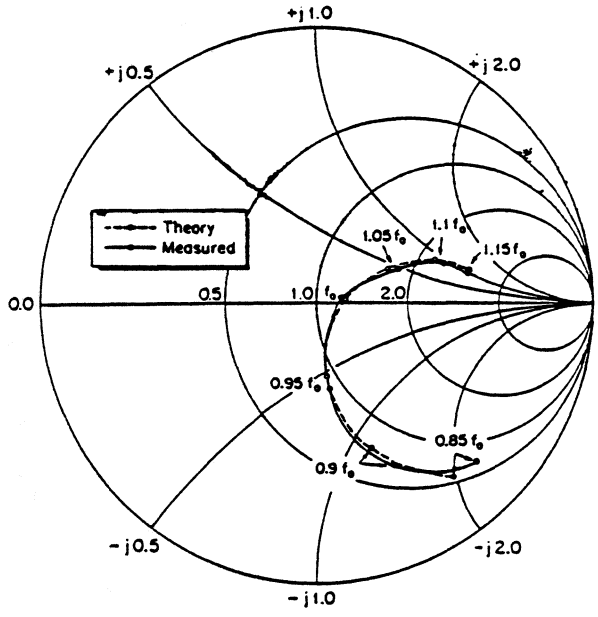

Figure 4: Predicted and measured dipole input impedance vs. frequency for a feed position of 0.41λ.

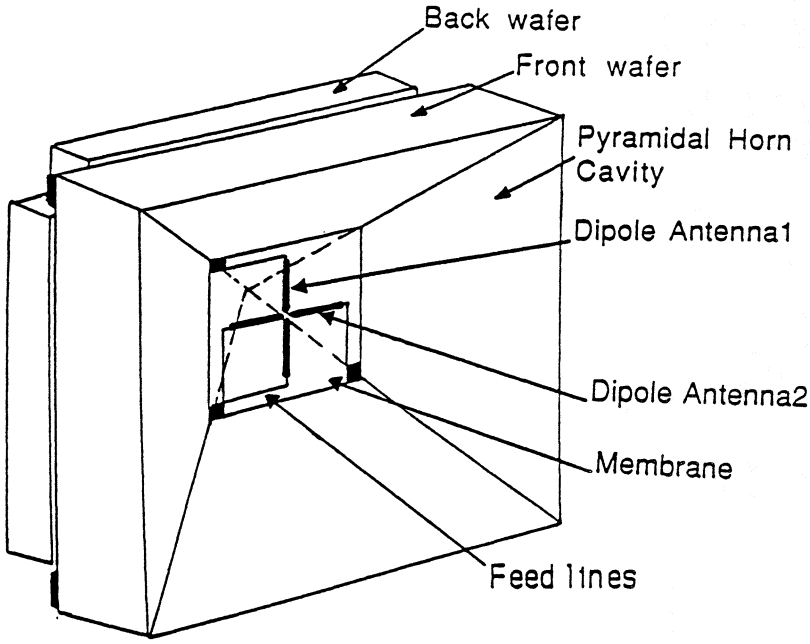

Figure 5: Monolithic dual-polarized horn antenna element with a novel bias and feeding structure.

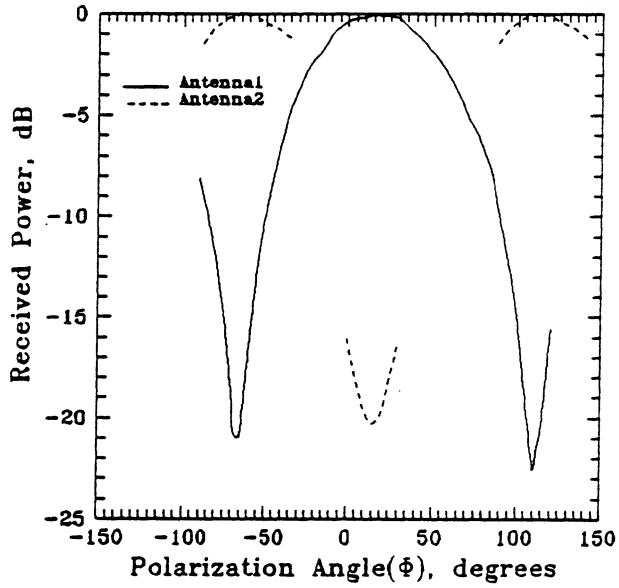

Figure 6: The measured polarization response of the orthogonal antennas at 92 GHz. The polarization isolation is better than -23dB.

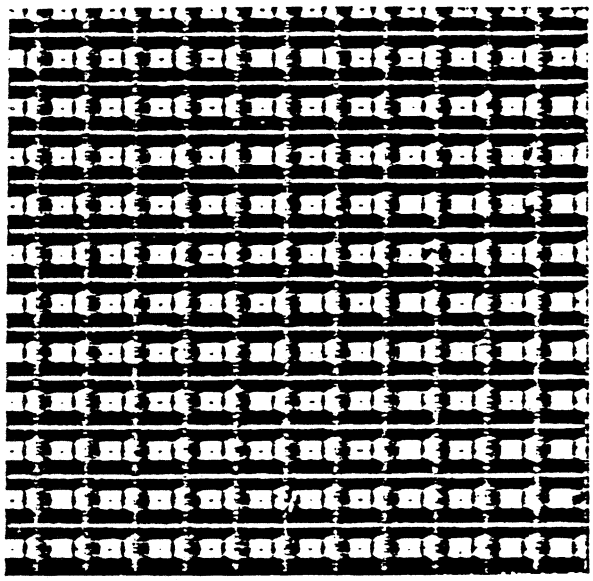

Figure 7: A 256-element two-dimensional horn imaging array at 802 GHz. The period of the array is 525μm and the horn aperture is 1.40λ.

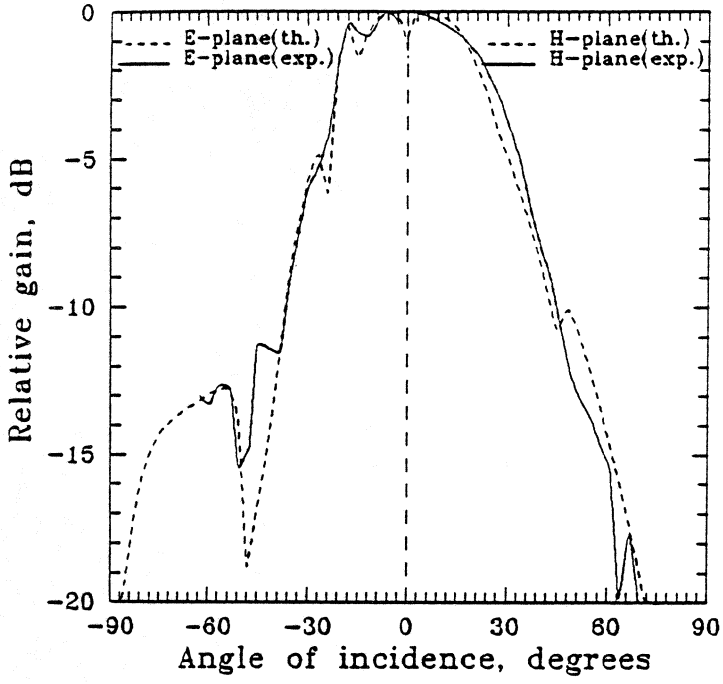

Figure 8: The measured theoretical and experimental E and H-plane patterns at 802 GHz.

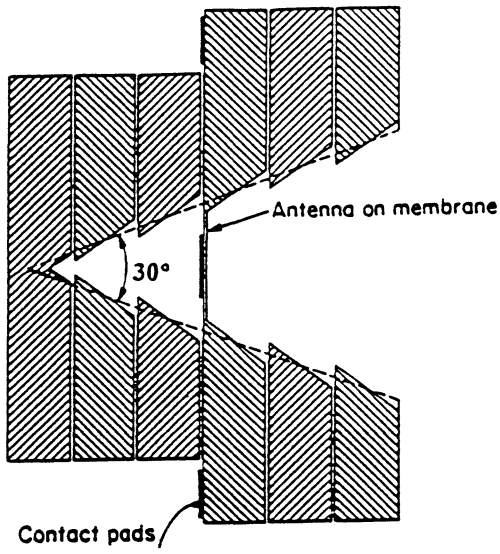

Figure 9: The step-profiled horn geometry (see text).

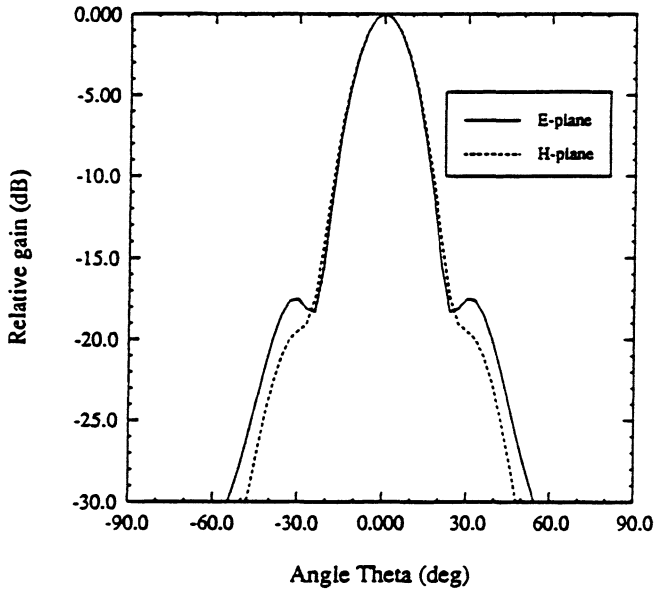

Figure 10: The calculated E and H-plane patterns for a step-profiled horn with an effective flare-angle of 30° and an aperture size of 2.92λ. The feeding dipole is positioned along the diagonal of the horn antenna.

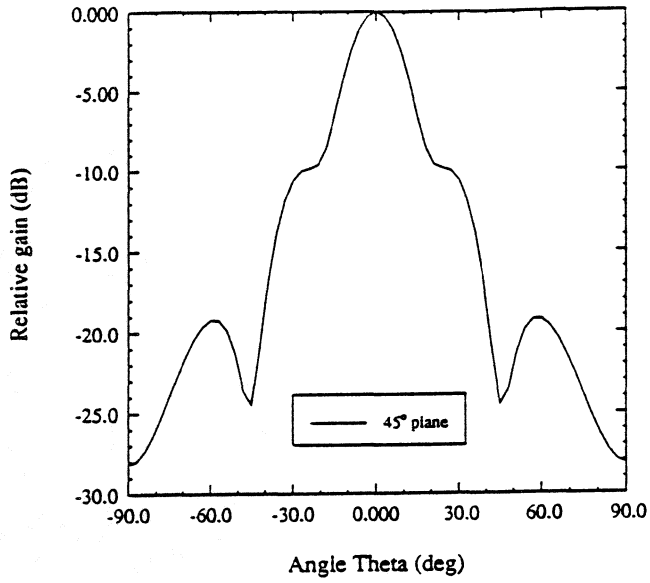

Figure 11: The calculated 45°-plane pattern for a step-profiled horn of figure 10.

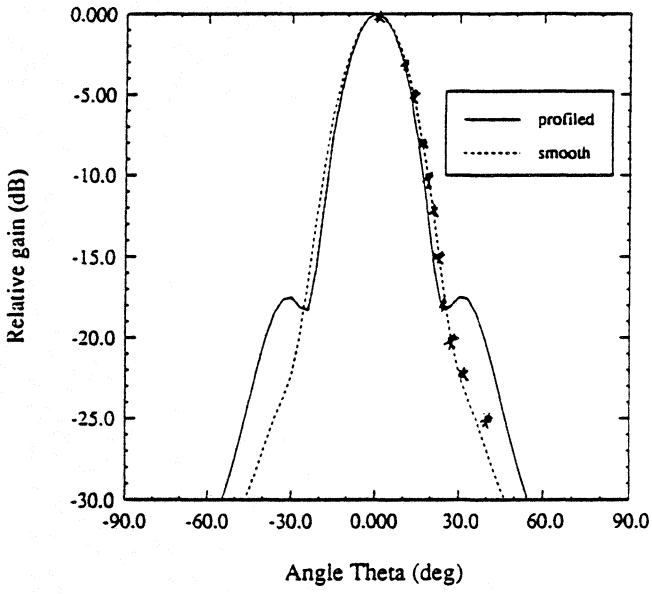

Figure 12: Comparison of the E-plane patterns between a step-profiled horn and its smooth counterpart. The crosses are measured points on a 12.1 GHz model.